Delta University Scientific Journal
Journal home page: https://dusj.journals.ekb.eg

Numerical validation on steel and stainless-steel girders under transverse monotonic loading

Yasmin Ali, Ahmed Elgammal

Civil Engineering Department, Faculty of Engineering, Delta University for Science and Technology, Gamasa, 11152, Egypt

Correspondence: Yasmin Ali; Gamasa 1152, Egypt; Tel: +20502770140; Fax: +20502770140; Email: yasmin.ali@deltauniv.edu.eg

ABSTRACT
Steel and stainless-steel girders are widely used around the world. However, relying solely on experimental testing of these girders is not always ideal since numerical simulations can also be utilized. Although experimental tests provide accurate results, numerical simulations offer several potential advantages. For example, they require fewer resources, including human, financial, and material resources. Moreover, numerical simulations can be applied to a broader range of structural parameters and loading conditions. Nonetheless, it is crucial to conduct a verification study before carrying out any numerical simulations to ensure that the developed numerical model accurately captures the actual behavior of the girder. Consequently, this research aims to verify the accuracy of finite element models of girders created in Ansys Workbench (2020 R1) by comparing them to experimental results from previously tested girders found in literature. The verification study uses models of specimens from different sources, including specimens made of stainless-steel, specimens with hollow tubular flanges, and stainless-steel girders with diagonal stiffeners. It is found that the finite element model can predict the ultimate strength and elastic stiffness of the girders with an average error of less than 3 and 0.4% respectively. Additionally, the model is able to simulate the deformed shape of the girders at the failure stage. Overall, the study demonstrated that the finite element model is effective at predicting the response of girders with different characteristics.

Keywords: *Steel; Stainless-steel; Girder; Beam; Transverse loading; Finite element.*

1. Introduction

In metallic structures, longitudinal elements are needed to carry the in-plane transverse loading resulting from the upper slab or covering system. In this regard, girders with I-shaped cross-sections, consisting of a web and two flanges, are utilized to play this role. The reason for commonly choosing such cross-section is its compatibility with the induced normal stress distribution caused by the acting loads. Moreover, the acting shear forces, mainly resisted by the web, are usually lower than the axial forces induced by the bending moments that are resisted by the flanges. This justifies the fact that the thickness of the webs is conventionally less than that of the flanges. When rigidity of a girder is not sufficient to resist the acting loads, transverse or longitudinal stiffeners can be equipped to the web panel. These stiffeners increase the rigidity of the web panel and divide it into several sub-panels. This prevents the web and flanges from buckling out-of-plane, and warping, respectively (Hasan et al., 2017). Transverse stiffeners are welded at certain equal spacings along the girder length. The end-post is the only exception as the transverse stiffeners spacing there may be different to fabricate different end-post configurations. Although steel is the most common metal used for the fabrication of such girders, several researchers also have indicated that stainless-steel can be used instead due to its durability, sustainability, and corrosion resistance. Moreover, the web of a girder is not always kept plain. In other words, it may be provided with web openings to accommodate for services such as pipes, cables, etc. (Amrous et al., 2023).

To increase the strength of a girder, the concrete slab can be linked to its top using shear connecters. If the interaction between the flange and slab is sufficient, composite action is thus developed and a composite girder is obtained. The latter is commonly characterized with better performance than individual girders. In general, the number of shear connectors decide whether the interaction is full or partial. In addition, the interaction state governs the strength of the composite girders (Hasan et al., 2017).

Another configuration of conventional girders is the corrugated girders. They consist of two flange plates and a corrugated that noticeably enhance buckling resistance. The most common corrugated webs are is the trapezoid-shaped. Compared to traditional girders with flat webs, a corrugated web girder allows for the

adoption of thinner webs Accordingly, a higher load resistance can be attained for lower cost (El Hadidy et al., 2018).

Since the I-shaped cross-section is considered as an open section, I-section girders usually lack adequate lateral-torsional buckling resistance unless properly designed with sufficient torsional stiffness. One of the methods to overcome this is to replace flat flanges of the girder by tubular ones. This causes the cross-section to transform from being open to closed cross-section which surely results in an increase in the torsional stiffness and lateral-torsional buckling resistance (Tondini & Morbioli, 2015; Ali et al., 2021; Ali, 2022).

Studies on steel girders has started a long time ago. (Wilson, 1986) reported that girders with slender webs exhibit stable deformability even after buckling propagation. Around 100 years later, several researchers developed design theories for the prediction of the ultimate strength of the girders that have been commonly named as the tension-field theories (Basler, 1961; Höglund, 1973, 1997; Porter et al., 1975; Dubas et al., 1985). Later, several studies have been directed towards the investigation of the behavior of girders under different loading conditions. (Azizinamini et al., 2007) studied the modes of failure of hybrid girders with different web slenderness ratios. (Vimonsatit et al., 2007) carried out tests on girders at elevated temperature. On the other hand, (Estrada et al., 2007a, 2007b; Real et al., 2007) experimentally tested I-section stainless-steel girders with different end-post configurations. (Chen et al., 2018) also dealt with the same point.

Furthermore, different models to predict the shear strength of girders have been suggested in literature. (White and Barker, 2008), based on extensive experimental testing, developed a tension field model to predict the shear resistance of girders. Design equations for shear resistance were also proposed by (Lee et al., 2008). (Ziemian, 2010) carried out an assessment study to check the accuracy of different available design models against test results found in literature. (Sinur and Beg, 2013a, 2013b) investigated the shear-moment interaction issue and compared the test results with those obtained from codes of practice methods. In another study similar in methodology, (Zhu and Zhao, 2015) compared experimental and numerical results, in which the effect of geometric imperfections and residual stresses were considered, with those obtained from different codes of practice. Moreover, (Kim and Uang, 2015) experimentally tested the shear resistance of steel and steel-concrete composite girders. Also, several well-known design models found in literature were evaluated by (Daley et al., 2017) against the strength of 27 experimentally tested unstiffened girders. (Kwon and Ryu, 2016) studied the effect of web slenderness, flanges stiffness, and end-post rigidity on the design strength of girders. Novel design method was also proposed. By conducting a series of experimental tests, (Hanses, 2018) design a plastic analytical design model for strength prediction of girders.

Recently, (Elgammal and Ali, 2022) numerically investigated dual web girders. (Shao et al., 2020; Elkawas, 2021) studied the lateral-torsional buckling of corrugated web girders. (Ali & Elgammal, 2022, 2023) suggested to equip flat webs containing openings with additional longitudinal stiffeners to enhance resistance to cyclic loading. (El-Boghdadi et al., 2023) demonstrated that diagonal stiffeners can be combined with transverse one in the same hollow flange girder to enhance its shear strength. (Pillali et al., 2023) carried out a fatigue life assessment for a composite girder. Moreover, (Chen et al., 2023a, 2023b; Kucukler, 2023) comprehensively tested stainless-steel girders.

Summing up, it can be deduced that steel and stainless-steel girders are commonly used and investigated worldwide. However, experimental testing of these girders should not be adopted alone; numerical simulations can be also used. In spite of the accuracy obtained from experimental tests, numerical simulations possess numerous potential advantages. For instance, less human, money, and material resources are needed in numerical simulations. Additionally, numerical simulations can be applied to a wider range of structural parameters and loading conditions. Nevertheless, a verification study should be carried out before any numerical simulations in order to evaluate the accuracy of the developed numerical model in capturing the actual behavior of the girder. So, this research presents general remarks related to the process of numerically modeling girders using the finite element software Ansys Workbench (2020 R1) (Ansys Inc., 2020). Subsequently, a verification study is carried out to compare the numerical obtained results with experimental results reported in literature for a series of experimental tests. The accuracy of the developed numerical models is also evaluated.

2. General overview on the finite element modeling

2.1. Definition of finite element analysis

Finite element analysis is a numerical technique which can be adopted to investigate numerous problems in nature (particularly engineering in the current research). In the finite element analysis, Structural Elements are divided into smaller elements. Stiffness matrix is developed for each of those elements then the full solution of

the whole structural element is attained by combining the individual solution of each single element, taking into account the continuity at the edges of the element.

2.2. The finite element software Ansys Workbench (Ansys Inc., 2020)

Ansys software (Ansys Inc., 2020) is considered as an advanced software package that can be utilize to model the interaction of several disciplines like physics, structural analysis, vibration, fluid dynamics, heat transfer and electromagnetic for engineers. In order to undergo relatively simple experience and user friendliness, the graphical user interface version of Ansys, called Ansys Workbench (Ansys Inc., 2020) is used. Ansys Workbench (Ansys Inc., 2020) has various features such as:

1) Suitable for both linear and nonlinear analyses.
2) Capable to model different objects in both two and three dimensions.
3) Extensive material library containing several predefined metallic alloys.
4) A complete set of elements including wide range of beam, shell (surface) and solid elements.
5) Ability to model contact among different bodies and elements.

2.3. Steps for the finite element analysis of steel and stainless-steel beams

In order to model metallic girders in Ansys Workbench (Ansys Inc., 2020), both material and geometric properties should be defined. To obtain accurate results, the finite element analysis should pass in two steps since metallic beams are predicted to be suspectable to buckling. The first step is concerned with the buckling modes of the girder through the Eigenvalue buckling analysis module. This type of analysis is considered as a linear elastic analysis which yields any desired number of buckling modes of the beam under consideration. However, only the first positive buckling mode is needed for the next step of the finite element analysis in which it is imported into the perfect geometry of the girder (Hassanein & Kharoob, 2013a). Subsequently, a nonlinear load-displacement analysis was carried out on the girders having initial geometric imperfections imported from the previous step leading to a set of results (e.g., load-displacement response, ultimate loads, modes of failure, etc.).

3. Finite element modeling of steel and stainless-steel beams

3.1. Geometry

For the numerical tests conducted in the current research, all of the girders were modelled in Ansys Workbench (2020 R1) (Ansys Inc., 2020) finite element software in full-scale since the isolated web panel simulation model does not accurately capture the response of plate girder web plates (Alinia et al., 2009).
Both of the girders and the equipped stiffeners were modelled using SHELL181 element which is a first-order structural shell element comprising four nodes with six degrees of freedom for each, thus it provides accepted solution for most applications and allows for shear deformation (Lee, 2023). In its ordinary shape, the SHELL181 element is quadrilateral but it can degrade to form a triangle, as shown in Fig. 1.

3.2. Material

The material of the girders was modeled as a von-Mises material with isotropic hardening (Hassanein & Kharoob, 2010; Ali et al., 2021). If the material to be used has its properties and stress-strain curve well-described in previous researches, its stress-strain curve could be modelled as a multilinear isotropic hardening curve (Fig. 2(a)). Note that this particular scheme of curves is defined in Ansys Workbench (Ansys Inc., 2020) as a relationship between plastic strain and true stress. On the other hand, in the case that the material stress-strain curve was not provided in literature, the multilinear isotropic hardening material model could be degenerated to a bilinear curve (Fig. 2(b)) composed of two segments only, as recommended by (EN 1993-1-5, 2004).

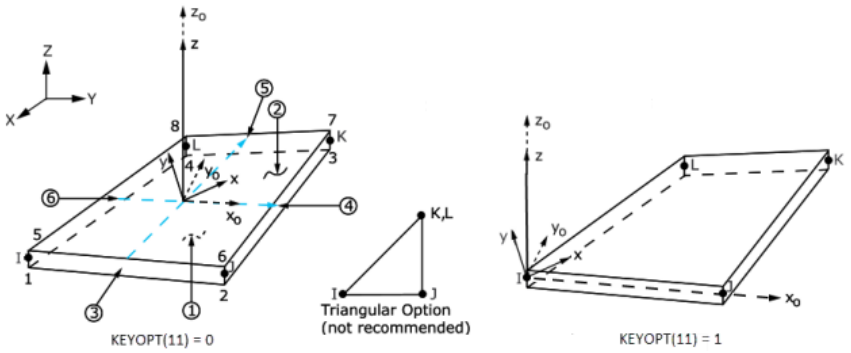

Fig. 1. General prospective of the SHELL181 element.

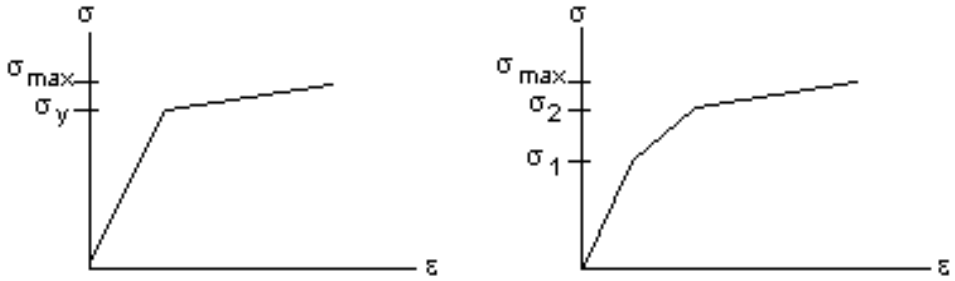

Fig. 2. Bilinear stress-strain curve (left) and multilinear stress-stain curve (right).

3.3. Boundary conditions

For all of the girders in the current research, the applied boundary conditions were taken following the numerical studies conducted in (Hassanein & Kharoob, 2010; Ali et al., 2021; Ali, 2022) in which the girder was loaded as a simply supported girder with/without end-posts. In detail, referring to Fig. 3, at each end of the girder, the midpoint of the web was restrained from translation in y-direction ($v_y = 0$), all web was restrained from translation in x-direction ($v_x = 0$), the flanges were restrained from rotation about z-axis ($R_z = 0$), and the central point of the bottom flange was restrained from translation in z-direction ($v_z = 0$). Moreover, the load was applied using a displacement control method in order to enable the capture of the strength loss phase in the load-displacement curves.

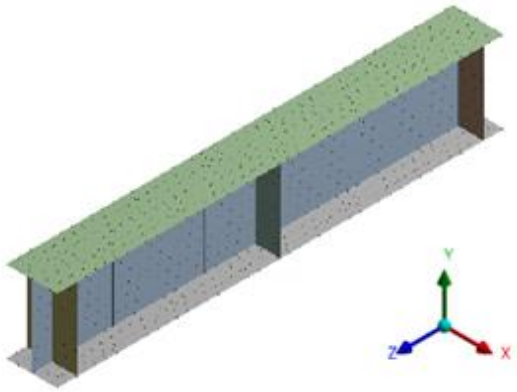

Fig. 3. Finite element model for a typical I-section girder.

3.4. Geometric imperfections and residual stresses

For all of the girders in the current research, initial geometric imperfections were considered in the finite element model by conducting linear Eigenvalue buckling analysis in order to obtain the first positive buckling

mode which was then scaled to a value of $L/1000$ (Hassanein & Kharoob, 2010, 2013b) wherein L denotes the span length of the girder, and then imported back into the perfect geometry of the girder in the nonlinear analysis step (Wang et al., 2020). In the Eigenvalue buckling analysis, there is no need to turn on the large deflection option, since this step relies on linear analysis approach. On the contrary, large deflection option should be turned on in the following loading steps in order to accumulate for nonlinear geometry effects. In regard to the residual stresses, they were neglected according to (Dong & Sause, 2009) for unbraced lengths less than 20 m. This condition is true for all of the girders under consideration in this research.

4. Verification study

4.1. Methodology of the finite element model validation

For the sake of obtaining accurate results in future studies on metallic girders, it is necessary first to check the accuracy of the current finite element model against the results of experimental tests available in literature. Accordingly, in the following subsections, three stainless-steel I-section plate girders of (Real et al., 2007), two hollow flange steel beams of (Tondini & Morbioli, 2015) and two diagonally stiffened stainless-steel I-section plate girders of (Yuan et al., 2019) were selected for the undergoing verification study. The load-displacement curves, load-carrying capacities, and modes of failure (if available) reported by the experimental tests were compared to those obtained from the finite element simulations.

4.2. Stainless-steel specimens of (Real et al., 2007) with transverse stiffeners

The current finite element model was verified herein via the simulation of stainless-steel I-section plate girders, labelled as ad1w4, ad15w4, and ad2w4, which were both experimentally and numerically tested by (Real et al., 2007). All of the three specimens shared several properties. In detail, they all had a web height of 500 mm, a web thickness of 4 mm, and a flange and stiffeners thickness of 20 mm. The only difference between the three specimens was their span length and stiffener spacing. ad1w4, ad15w4, and ad2w4 had span lengths of 1, 1.5, and 2 m, respectively, and stiffener spacings of 500, 750, and 1000 mm, respectively. It is worth pointing out that the flange width and edge distance of the plate girders were not clearly mentioned in the paper; however, they were assumed herein to be equal to 250 mm and 100 mm, respectively. The used material was austenitic stainless-steel grade 1.4301 (AISI 304) which has a modulus of elasticity of 197240 MPa and 187340 MPa for 4 mm and 20 mm thick plates, respectively, and a Poisson's ratio of 0.3. Since the stress-strain curves of that stainless-steel were clearly presented by (Real et al., 2007), they were modelled herein using a multilinear isotropic hardening model. The plate girders were modelled as being simply supported at both of their ends. The plate girders were also loaded at their midspan with a concentrated load so that the web was under constant shear. The load was applied at the intersection of the midspan transverse stiffeners and the upper flange. Fig. 4 illustrates the finite element models of the three plate girders under consideration.

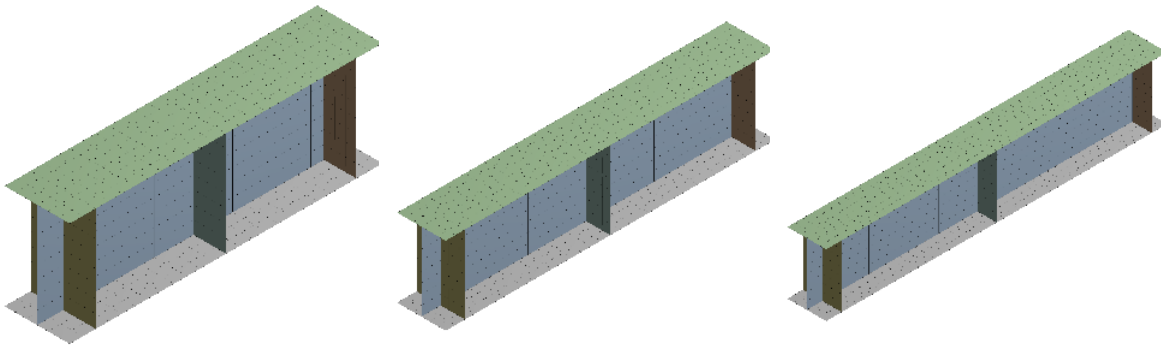

(a) ad1w4 (b) ad15w4 (c) ad2w4

Fig. 4. Finite element models for the specimens of (Real et al., 2007).

Figs. 5 to 7 depict the resulting load and midspan vertical displacement for both of the experimental tests and the current finite element modelling. The ratio between the finite element ultimate load and the experimental ultimate load for specimens ad1w4, ad15w4, and ad2w4 were found to be 1.03, 1.07, and 1.0, respectively. Moreover, the ratio of the finite element elastic stiffness to the experimental elastic stiffness was 1.02, 0.97, and 0.93 for ad1w4, ad15w4, and ad2w4, respectively. It can be detected that the finite element results followed a trend similar to that of the experimental results but having somehow higher ultimate load. Nevertheless, that difference was small and still within the acceptable limits.

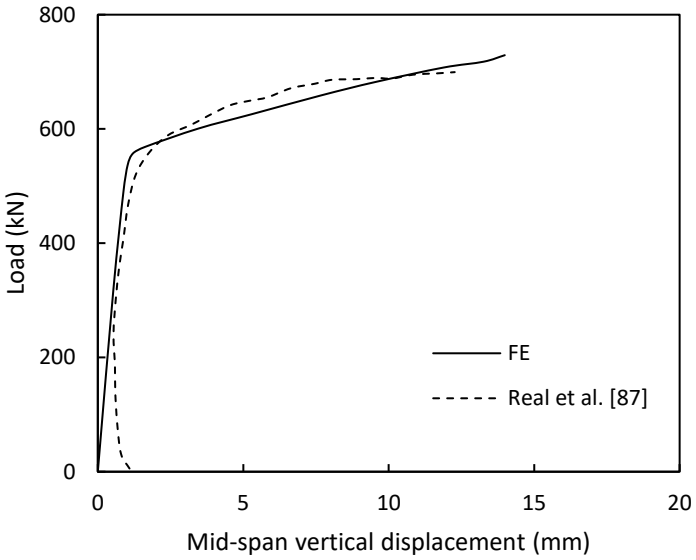

Fig. 5. Load-displacement curves for ad1w4.

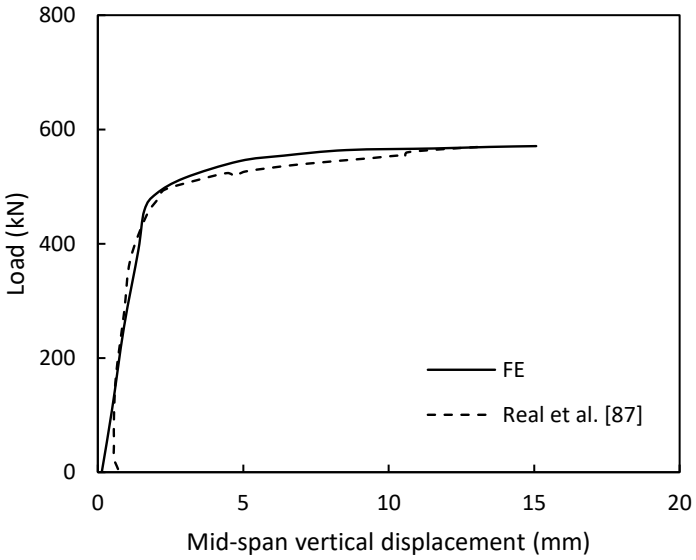

Fig. 6. Load-displacement curves for ad15w4.

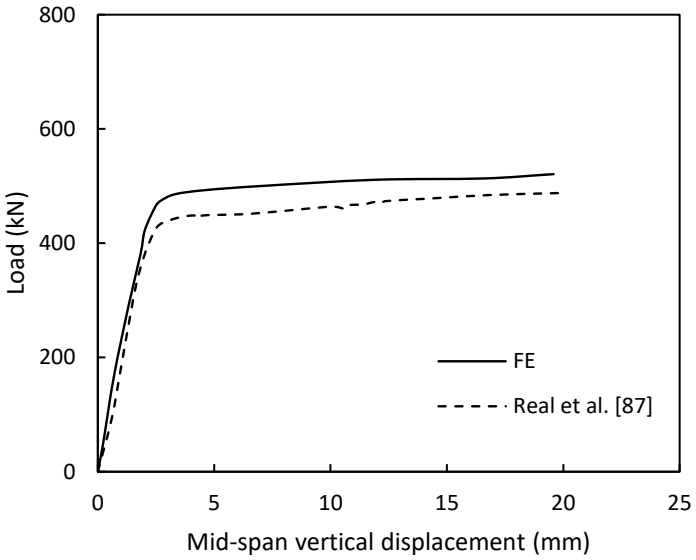

Fig. 5. Load-displacement curves for ad2w4.

4.3. Steel specimens of (Tondini & Morbioli, 2015) with transverse stiffeners

(Tondini & Morbioli, 2015) analysed the strength and response of steel rectangular hollow flange beams in order to be used in small steel frames. Two laterally restrained hollow flange beams of different geometric characteristics with three specimens for each beam were experimentally. The yield and ultimate tensile stresses of the used material were 274.1 and 354.4 MPa for the web, and 343.3 and 391 MPa for the flat regions of the flanges, respectively. The enhanced yield stress value in the corner regions of the tubular flanges, resulting from cold-forming process, was not included in the finite element analysis since its enhancement is countered by the existence of the compressive membrane residual stresses (Schafer & Peköz, 1998). The actual stress-strain curve of the used material provided by (Tondini & Morbioli, 2015) was used; it was modeled as a multilinear isotropic hardening curve as discussed earlier. The load was applied concentrically on the edges of the double-sided mid-span stiffeners to reduce the local loading effects on the tubular flanges. Table 1 lists the geometric characteristics of the specimens while Fig. 6 presents the finite element models for each specimen.

Table 1. Geometric characteristics of (Tondini & Morbioli, 2015) specimens (unit: mm).

Specimen	Web height	Flanges width	Flanges depth	Web & flanges thickness	Span-length
T03 RHFB-240	195.9	99.9	19.7	2.01	4495
T06 RHFB-300	237.1	150.1	30.2	2.93	4498

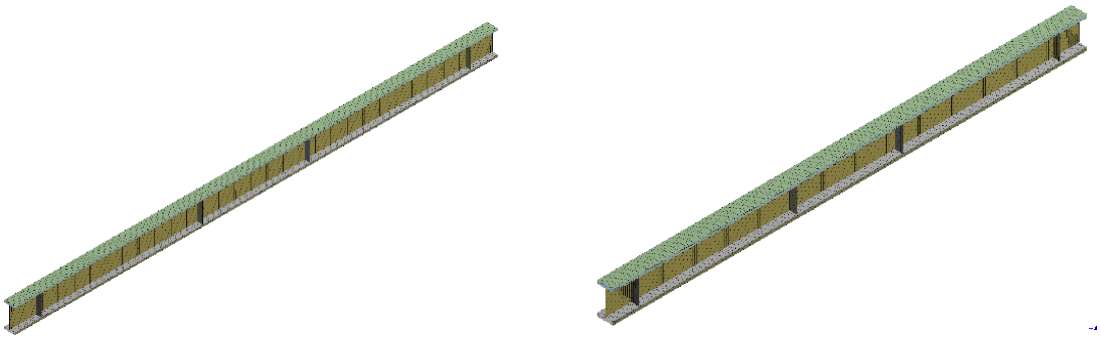

Fig. 6. Finite element models for T03 RHFB-240 (left) and T06 RHFB-300 (right).

The ultimate moment and the midspan vertical displacement at the step of the maximum load-carrying capacity were attained from the finite element simulations then compared with the corresponding experimental test

results. It is found that the finite element model yielded accurate results as the ratio of the finite element ultimate moment to the experimental ultimate moment was 1.04 and 1.05, respectively, for RHFB-240 and RHFB-300. On the other hand, finite element elastic stiffness to the experimental elastic stiffness was 1.07 and 1 for the same specimens, respectively. Fig. 7 displays a comparison of the finite element and experimental moment-midspan vertical displacement curves for the beams. Both numerical and experimental curves appeared to look alike with minor deviations especially for RHFB-240. That deviation in the stiffness between the numerical and experimental curves is caused by the existence of geometric imperfections which were not measured by (Tondini & Morbioli, 2015) while, at the same time, the used maximum imperfection suggested by (Hassanein & Kharoob, 2010) was relatively smaller than the actual one. It is thus evident that the finite element model accurately predicted the ultimate moment, elastic stiffness, and the general shape of the moment-midspan vertical displacement curves.

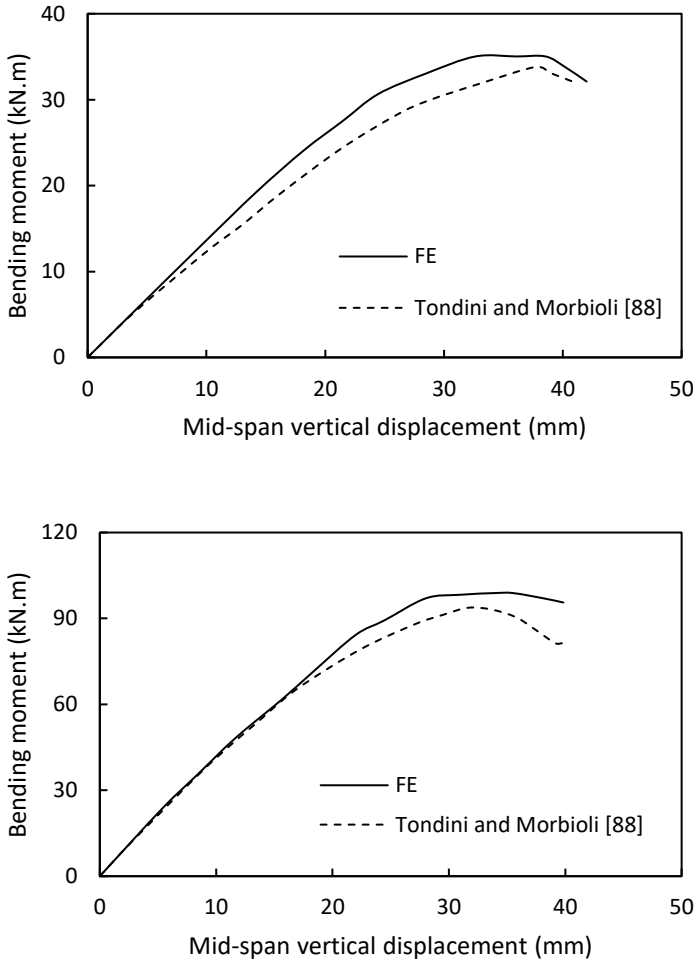

Fig. 7. Moment-midspan vertical displacement curves for T03 RHFB-240 (top) and T06 RHFB-300 (bottom).

4.4. Stainless-steel specimens of (Yuan et al., 2019) with diagonal stiffeners

The experimental program of (Yuan et al., 2019s) included four I-section stainless-steel plate girders; only two of them were installed with diagonal stiffeners. Accordingly, these two were the only specimens of concern since transversely stiffened girders and beams were sufficiently validated throughout the current section. General Characteristics of the two specimens are listed in Table 2. One of the specimens (V-304-DF) was made of stainless-steel grade EN 1.4301, while the another one was made of the grade EN 1.4462. Overall, (Yuan et al., 2019) provided the stress-strain curve, for both grades, obtained from experimental coupon testing. So, these curves were used to model the material using the multilinear isotropic hardening curve, as discussed earlier.

Table 2. Geometric characteristics of (Yuan et al., 2019) specimens (unit: mm).

Specimen	Material	L	a	e	h_w	b_f	t_w	t_f	t_s	t_{ds}	b_{ds}
V-304-DS	1.4301	1696.6	748.3	100.1	498.4	150	3.82	11.85	7.85	3.82	29.7
V-2205-DS	1.4462	1697.8	749.1	99.8	498.2	150.2	3.9	12.59	7.72	3.90	29.9

e is the end-post edge distance, t_s is the transverse stiffener thickness, t_{ds} is the diagonal stiffener thickness, and b_{ds} is the diagonal stiffener width.

In Fig. 8, the relationship between shear resistance and midspan vertical displacement obtained from the finite element analyses is plotted, for both specimens, along with those of the experimental tests. Obviously, great agreement exists between the finite element and experimental shear response. Furthermore, the ratio of the ultimate shear resistance obtained from the current finite element model to that of the experimental test was 1.02 and 1.01 for V-304-DS and V-2205-DS, respectively. With regard to the elastic stiffness, its numerically-obtained value to the experimentally-obtained one was 1.03 and 1.01 for the same two specimens, respectively. In the same vein, the deformed shape of the specimens at failure was identical for both the finite element analysis and the experimental test, as shown in Fig. 9. That way, the accuracy of the developed finite element model in capturing the response of diagonally stiffened girders was also verified.

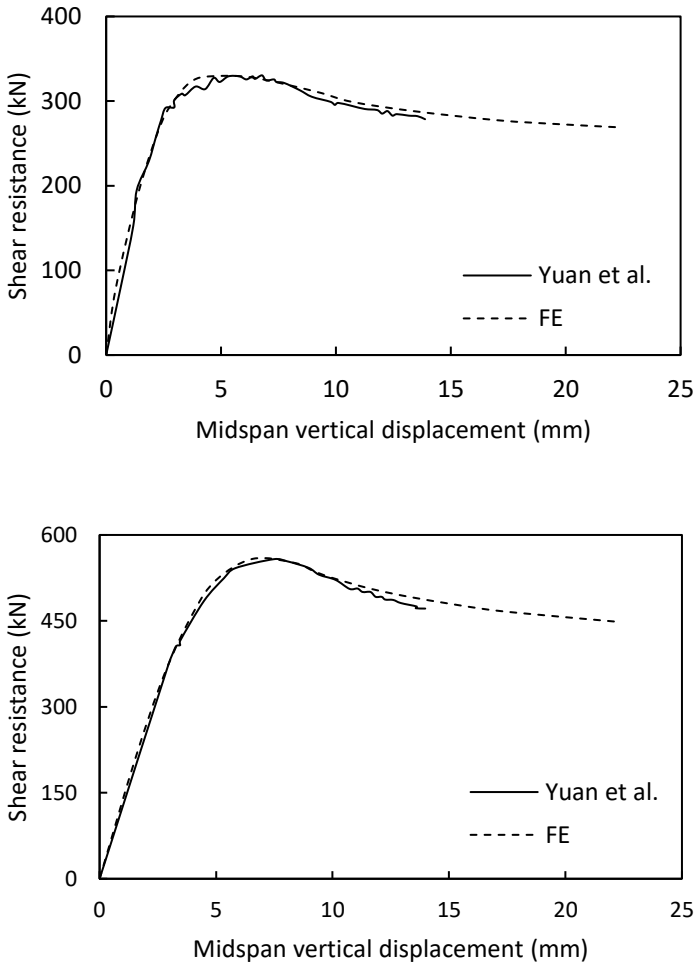

Fig. 8. Shear response of V-304-DS (top) and V-2204-DS (bottom)

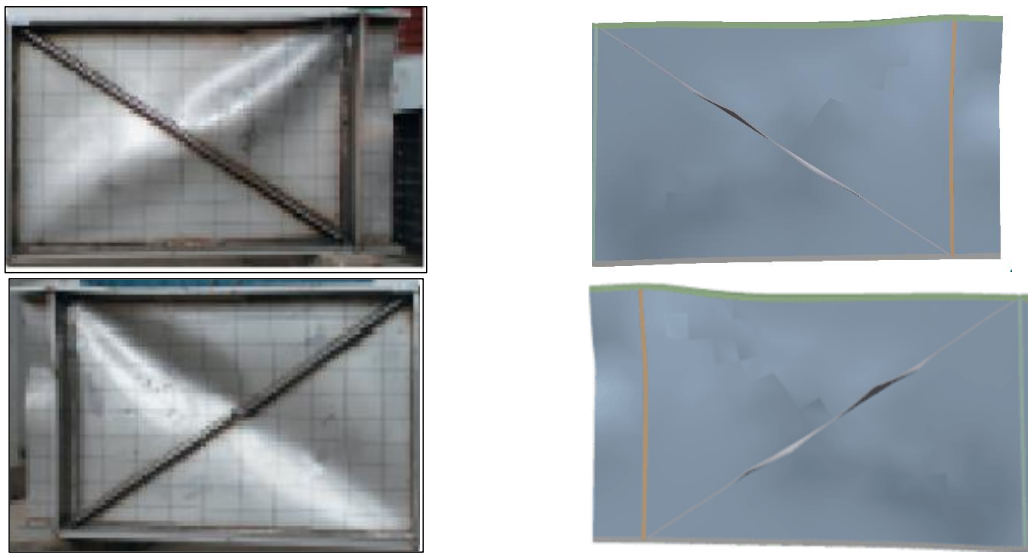

Fig. 9. Comparison between test and finite element deformed shapes of V-304-DS (top) and V-2204-DS (bottom) at the step of failure.

5. Summary

In this research, a verification study was conducted to check the accuracy of the finite element models of girders, built in Ansys Workbench (2020 R1) (Ansys Inc., 2020), in capturing the response of early experimentally tested girders found in literature. The verification study mainly depended on building models for certain specimens of (Real et al., 2007; Tondini & Morbioli, 2015; Yuan et al., 2019) and then validated them against the experimental results provided by them. The verification study included a wide variety of beams and girders with different properties. For instance, (Real et al., 2007) specimens were made of stainless-steel, (Tondini & Morbioli, 2015) specimens were provided with hollow tubular flanges, and (Yuan et al., 2019) stainless-steel girders were equipped with diagonal stiffeners.
It was found that the developed finite element model can predict the ultimate strength and elastic stiffness of girders with an average error not exceeding 3 and 0.4%, respectively. Furthermore, the finite element model was also capable of simulating the deformed shape of the girders at the step of failure. To sum up, it is seen that the current finite element model can noticeably predict the response of girders with different characteristics.

Disclosure

The authors report no conflicts of interest in this work.

References

Ali, Y.; El-Boghdadi, M.; El Hadidy, A. Cyclic shear performance of hollow tubular flange plate girders: A numerical study. In: Proceedings of the International Conference on Advances in Structural and Geotechnical Engineering. Hurghada, Egypt, 2021.

Ali, Y. Behavior of hollow tubular flange plate girders subjected to cyclic loading. M.Sc. thesis. Tanta University, Tanta, Egypt, 2022.

Ali, Y.; elgammal, A. Compensating steel web-opened beams for the loss in cyclic shear capacity by longitudinal stiffeners. In: Proceedings of the International Engineering Conference on Research and Innovation. Cairo, Egypt, 2022.

Ali, Y.; Elgammal, A. Compensating steel web-opened beams for the loss in cyclic shear capacity by longitudinal stiffeners. Delta University Scientific Journal, 2023, 6.1: 123-134.

Alinia, M. M.; Shakiba, Maryam; Habashi, H. R. Shear failure characteristics of steel plate girders. Thin-Walled Structures, 2009, 47.12: 1498-1506.

Amrous, H.; Yossef, N. M.; El-Boghdadi, M. H. Experimental study and structural analysis of tapered steel beams with cellular openings. Engineering Structures, 2023, 288: 116212.

ANSYS, Inc. Ansys Workbench (2020 R1). Canonsburg, USA, 2020.

Azizinamini, Atorod, et al. Shear capacity of hybrid plate girders. Journal of Bridge Engineering, 2007, 12.5: 535-543.

Basler, Konrad. Strength of plate girders in shear. Journal of the Structural Division, 1961, 87.7: 151-180.

Chen, X.; Yuan, H. Local buckling behaviour of longitudinally stiffened stainless steel plate girders under combined bending and shear. Thin-Walled Structures, 2023, 184: 110541.

Chen, X.; Yuan, H.; Real, E. Bending-shear interaction buckling of stainless steel plate girders: Numerical investigation and design method. In: Structures. Elsevier, 2023. p. 2113-2128.

Daley, Aaron J.; Brad DAVIS, D.; WHITE, Donald W. Shear strength of unstiffened steel I-section members. Journal of Structural Engineering, 2017, 143.3: 04016190.

Dong, J.; Sause, R. Flexural strength of tubular flange girders. Journal of Constructional Steel Research, 2009, 65.3: 622-630.

Dubas, Pierre; Maquoi, R.; MASSONNET, Ch. Behaviour and design of steel plated structures. IABSE surveys, 1985, 31-85: 17-44.

El Hadidy, A. M.; Hassanein, M. F.; Zhou, M. The effect of using tubular flanges in bridge girders with corrugated steel webs on their shear behaviour–A numerical study. Thin-Walled Structures, 2018, 124: 121-135.

Elgammal, A.; Ali, Y. Shear strength of dual web plate girders with transverse stiffeners. Delta University Scientific Journal, 2022, 5.2.

Comité Européen De Normalisation (CEN). Eurocode 3: Design of Steel Structures - Part 1-5: Plated Structural Elements. Brussels, Belgium. 2004.

El-Boghdadi M.; El Hadidy, A.; Ali, A.; Elgammal, A. Parametric study of diagonally stiffened plate girders with compression hollow flanges under shear loading. In: Proceedings of the International Conference on Advances in Structural and Geotechnical Engineering. Hurghada, Egypt, 2023.

Estrada, I.; Real, E.; Mirambell, E. General behaviour and effect of rigid and non-rigid end post in stainless steel plate girders loaded in shear. Part I: Experimental study. Journal of constructional steel research, 2007, 63.7: 970-984.

Estrada, I.; Real, E.; Mirambell, E. General behaviour and effect of rigid and non-rigid end post in stainless steel plate girders loaded in shear. Part II: Extended numerical study and design proposal. Journal of Constructional Steel Research, 2007, 63.7: 985-996.

Hansen, Thomas. Post-buckling strength of plate girders subjected to shear–experimental verification. Steel Construction, 2018, 11.1: 65-72.

Hasan, Q. A., et al. The state of the art of steel and steel concrete composite straight plate girder bridges. Thin-Walled Structures, 2017, 119: 988-1020.

Hassanein, M. F.; Kharoob, O. F. Shear strength and behavior of transversely stiffened tubular flange plate girders. Engineering Structures, 2010, 32.9: 2617-2630.

Hassanein, M. F.; Kharoob, O. F. Behavior of bridge girders with corrugated webs:(II) Shear strength and design. Engineering Structures, 2013, 57: 544-553.

Hassanein, M. F.; Kharoob, O. F. Shear capacity of stiffened plate girders with compression tubular flanges and slender webs. Thin-Walled Structures, 2013, 70: 81-92.

Höglund, Torsten. Design of thin plate I girders in shear and bending with special reference to web buckling. Department of Structural Mechanics and Engineering, Royal Institute of Technology, 1973.

Höglund, Torsten. Shear buckling resistance of steel and aluminium plate girders. Thin-walled structures, 1997, 29.1-4: 13-30.

Kucukler, M. Shear resistance and design of stainless steel plate girders in fire. Engineering Structures, 2023, 276: 115331.

Kwon, Young Bong; Ryu, Seung Wan. The shear strength of end web panels of plate girders with tension field action. Thin-Walled Structures, 2016, 98: 578-591.

Lee, Sung C.; Lee, Doo S.; Yoo, Chai H. Ultimate shear strength of long web panels. Journal of Constructional Steel Research, 2008, 64.12: 1357-1365.

Lee, Huei-Huang. Finite Element Simulations with ANSYS Workbench 2023: Theory, Applications, Case Studies. SDC publications, 2023.

Porter, D. M.; HR, Evans. The collapse behaviour of plate girders loaded in shear. 1975.

Real, E.; Mirambell, E.; Estrada, I. Shear response of stainless steel plate girders. Engineering Structures, 2007, 29.7: 1626-1640.

Schafer, Benjamin W.; Peköz, Teoman. Computational modeling of cold-formed steel: characterizing geometric imperfections and residual stresses. Journal of constructional steel research, 1998, 47.3: 193-210.

Sinur, Franc; Beg, Darko. Moment–shear interaction of stiffened plate girders—Tests and numerical model verification. Journal of Constructional Steel Research, 2013, 85: 116-129.

Sinur, Franc; Beg, Darko. Moment–shear interaction of stiffened plate girders—Numerical study and reliability analysis. Journal of Constructional Steel Research, 2013, 88: 231-243.

Tondini, Nicola; Morbioli, Andrea. Cross-sectional flexural capacity of cold-formed laterally-restrained steel rectangular hollow flange beams. Thin-Walled Structures, 2015, 95: 196-207.

Wang, Y. M., et al. Prediction of flexural and shear yielding strength of short span I-girders with concrete-filled tubular flanges and corrugated web-II: Numerical simulation and theoretical analysis. Thin-Walled Structures, 2020, 148: 106593.

White, Donald W.; Barker, Michael G. Shear resistance of transversely stiffened steel I-girders. Journal of Structural Engineering, 2008, 134.9: 1425-1436.

Wilson, Joseph M. On specifications for strength of iron bridges. Transactions of the American Society of Civil Engineers, 1886, 15.1: 389-414.

Yuan, H. X., et al. Shear behaviour and design of diagonally stiffened stainless steel plate girders. Journal of Constructional Steel Research, 2019, 153: 588-602.

Zhu, Y. Y.; Zhao, J. C. Experimental study and numerical simulation on steel plate girders with deep section. In: 6 th International Conference on Advances in Experimental Structural Engineering, 11 th International Workshop on Advanced Smart Materials and Smart Structures Technology. 2015. p. 1-2.

Ziemian, Ronald D. (ed.). Guide to stability design criteria for metal structures. John Wiley & Sons, 2010.